Available online at www.sciencedirect.com

ScienceDirect

Procedia Structural Integrity 24 (2019) 267–278

Structural Integrity Procedia

www.elsevier.com/locate/procedia

AIAS 2019 International Conference on Stress Analysis

Optical Method to measure mesh tensioning

Lorenzo Beretta[a], Emanuele Marotta[a], Pietro Salvini[a]*

[a]*Department of Enterprise Engineering, University of Rome "Tor Vergata", via del Politecnico, 1 00133 - Rome - ITALY*

Abstract

The present paper presents a method to estimate the tensional status of a knitted mesh. To reach this result, the relationship between the frequencies of vibration, recorded by a high-sampling camera and analysed through image processing, and different tensioning on the mesh itself, has been investigated.
After having conducted several tests, all the collected pairs frequency-tensional status have been used to extrapolate an optimal (in a least-squares sense) correlation between frequency of vibration and tension of the mesh.

Keywords: Net Vibrations; Net Stress Measurement; Image Processing

1. Introduction

In the last decades, new types of antenna for satellites have been developed. Among them, particular interest is given to AstroMesh® Reflectors, made up of large deployable reflector (LDR), see Fig. 1. They consist in a particular mesh of gold-plated tungsten or molybdenum wires, stretched over a circular low-weight support, and forced so that to approximate a paraboloid shape by two nets, as shown in Fig. 2. What makes the AstroMesh® Reflector so suitable for space missions are their characteristics of extraordinary low weight accompanied by a high stiffness, thermal stability and optimal performance in radio frequency reflectivity, Thomson (2000).

The study aims to check the two-dimensional tensioning status acting on the mesh, which must be kept in a defined

* Corresponding author. Tel.: +39.06.7259.7140; fax: +39.06.7259.7145.
E-mail address: salvini@uniroma2.it

10.1016/j.prostr.2020.02.024

range of values so that the reflector can fulfill its function by assuring appropriate contact between wires.

The procedure here adopted consists in experimental evaluation of the tensional status through the analysis of high sampling frequency videos of both free and forced vibrations of a mesh sample, taking advantage of the relationship between tension and transverse vibration frequencies. (A transverse vibration is that one in which the small displacement of any point is perpendicular to the plane of the mesh in its reference configuration, i.e. that of equilibrium).

Of all the existing mesh reflector constructive technologies, the current state-of-the-art for demonstrated on-orbit stability and surface accuracy is AstroMesh® reflector, whose aperture, at present, ranges from 3 to 50 meters and above in diameter, depending on the model Northropgrumman (2012), Northropgrumman (2017).

As shown in Fig. 2, the main components of an AstroMesh® reflector are a flat deployable perimeter truss, front and rear nets, tension ties, and the mesh (in yellow in the picture).

Fig. 1. AstroMesh® Reflector (https://news.northropgrumman.com).

The front and rear nets are composed of composite web elements presenting near-zero-CTE (Coefficient of Thermal Expansion), that form two back-to-back domes. The front net is shaped to approximate the required parabolic surface with triangular facets: the smaller they are, the better the approximation is Northropgrumman (2012). The webs are tensioned to relatively high-stress levels by the application of normal loads from tension ties. These high-stress levels allow the front net to maintain very high stability and shape precision, despite negligible parasitic mesh loads.

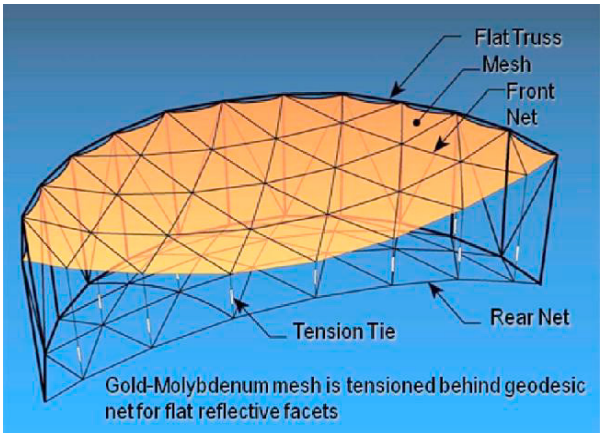

Fig. 2. Schematic view of the AstroMesh reflector (taken from Thomson et al. (2007)).

The perimeter truss is composed of near-zero-CTE carbon fiber composites as well, conferring to the whole structure his high stiffness and thermal stability.

The mesh here considered is made of extremely fine gold-plated tungsten wires and their high elasticity allows them to yield the structural parabolic shape provided by the front net. Thanks to its excellent RF (Radio Frequency) Reflectivity, it points the desired electromagnetic signal to the specific direction. Other noteworthy advantages of using a Deployable Reflector are its capability to be packaged in an extremely small volume, its extremely low areal mass, its high stability and longevity in a space environment Thomson et al. (2007), Thomson et al. (2008).

The present study focusses on the reflective mesh. In particular, the aim is devoted to finding a simple, easy to repeat and non-destructive way to estimate the effective tension value in each direction of the plane.

Knowing the effective tensioning is vital since it must be, Marotta et al. (2016):

- Low enough to be negligible compared to the tension of the nets and to not provoke excessive stresses in the mesh, avoiding permanent plastic deformations due to the wide thermal range encountered in the environmental space conditions;
- High enough to make the mesh adherent to the net and to ensure contacts among wires of the mesh itself so that RFF is optimal.

Briefly, the tension status must be maintained between these two former bonds. Besides, this range can be even more limited, considering the fact that tensioning has an impact on the shape and size of the openings among wires, thus affecting the RFF reflectivity of the mesh, De Salvador et al. (2018).

Since a vibrating structure (one, two or three-dimensional) presents a relationship between tension and vibration frequency(-ies), it was thought to induce vibrations in the mesh and correlate the frequency response to the applied tension. Physical structure models used for the tuning includes wires, membranes, and nets, with specific boundary conditions. Preliminarily, these models do not include some effects:

- Strong anisotropic behavior of the mesh across different directions;
- The Complexity of the pattern and of links among wires (as shown in Fig. 3);
- Viscous damping.

Finally, the real case has been studied and correlations between tension and vibration frequencies have been found out through experimental tests.

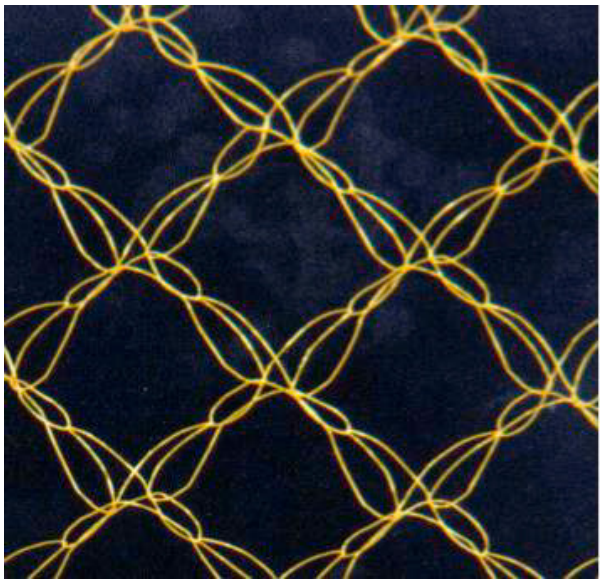

Fig. 3. Particular of the mesh geometry - Thomson et al. (2008).

2. Analytical models of one- and two-dimensional structures

Vibrating wire. Making the assumptions of uniform tension across the length of the wire and small displacements, a vibrating wire hinged at both extremities presents a simple relationship between tension and bending natural

frequencies:

$$\nu_n = \frac{n}{2L}\sqrt{\frac{T}{\rho}} \tag{1}$$

where T is the uniform tension, ρ is the linear density, L is the length of the wire and n refers to the n^{th} natural frequency.

Rectangular membrane. Assuming that the membrane is a perfectly flexible and infinitely thin lamina of uniform material and thickness, hinged at its boundaries, Weaver et al. (1990), uniformly stretched in its plane directions by a tension per unit of length so large that the fluctuation of this tension, due to the small deflections during vibration, can be neglected:

$$\nu_{m,n} = \frac{1}{2}\sqrt{\frac{S}{\sigma}\left(\frac{m^2}{a^2}+\frac{n^2}{b^2}\right)} \tag{2}$$

where σ is the uniform areal density, a and b the dimensions of the membrane, m and n identify the natural mode of vibration, S the uniform tension per unit of length (uniformity of tension is fundamental, otherwise shear stresses appear and an exact demonstration of that formula is much harder).

Rectangular net. The previous case can be extended to that of a net if two orthogonal resulting stresses are considered, and accounting that the shear stress is negligible whatever are the tensions applied (due to wire assembly, see Fig. 4)

$$\nu_{m,n} = \frac{1}{2}\sqrt{\frac{1}{\sigma}\left(\frac{m^2}{a^2}T'_x+\frac{n^2}{b^2}T'_y\right)} \tag{3}$$

where T'_x and T'_y are two uniform orthogonal tensions per unit of length.

Circular membrane. Under the same hypothesis of the rectangular membrane:

$$\nu_{m,n} = \frac{(\lambda a)_{m,n}}{2\pi r}\sqrt{\frac{S}{\sigma}} \tag{4}$$

where $(\lambda a)_{m,n}$ is a coefficient that identifies the natural mode of vibration, being the solution based on the zeros of the Bessel's function of the first type J_n, r is the radius of the membrane. The value of the $(\lambda a)_{m,n}$ coefficient must be defined, it does not account for the anisotropy of the net.

For the net here accounted and the experimental procedure later explained, the most interesting natural frequency is the first one. So it is sufficient to substitute in the previous formulas $n=m=1$ and $(\lambda a)_{m,n} \cong 2{,}404$.

3. Model approach for a vibrating mesh

In the previous paragraph, it is possible to notice a strong analogy between the formulas introduced for rectangular membranes and the net; substantially, they are the same, except for the presence in the net's formula of two tensions, rather than only one. This fact is due to the absence of shear stresses in a net (whose structure is representable as a series of hinges and flexible rods, as shown in Fig. 4) whatever the tension status is. On the contrary, if a membrane is loaded with different tensions (depending on the direction of load), a complex tensor of stress is established on the membrane and a simplified analytical approach to the problem of vibration is much less trivial.

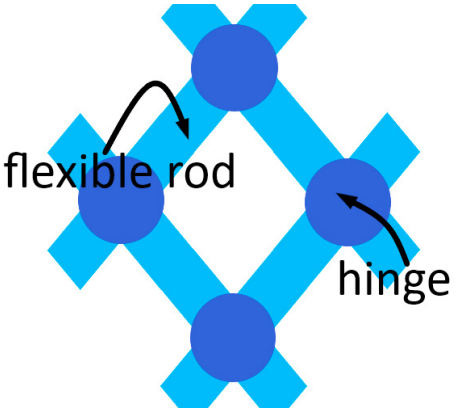

Fig. 4. Net mechanical scheme.

An analytic approach for the circular net does not exist in the literature; therefore, it was thought to apply the same analogy given for rectangular membranes, to obtain a non-exact, but right-minded, trend for the frequency of vibration of a circular net, when two orthogonal loads are present.

$$\nu_{m,n} = \frac{(\lambda a)_{m,n}}{2\pi r}\sqrt{\frac{T'_x + T'_y}{\sigma}} \tag{5}$$

Again, for the first natural frequency $(\lambda a)_{m,n} \cong 2{,}404$.

The present study focusses on transverse vibrations since it is a hard task to deal with the in-plane vibrations, even if studying these latter ones would have been much better for our goal. In fact, transverse vibrations extend up to the edges, thus being strongly influenced by the boundary conditions (the type of restraints and perimeter shape). The measurements here done refer to a hinged circular perimeter, but changing the boundary conditions means altering the frequency dependence from loads.

On the other hand, in-plane vibrations affect a much smaller area of the mesh and are virtually independent of the type of boundary (if the dimensions of the disturbed areas are reasonably small compared to those of the mesh, which was our case). Therefore, in-plane vibrations offer the possibility to get a broader universal formula, independent of the particular boundary conditions. Unfortunately, in-plane vibrations present the inconvenience of being much faster than the transverse ones, thus resulting in difficult to catch with the available photographic equipment. This is why in-plane vibrations have been omitted in this study.

4. Experimental results

4.1. Testing Machine

Because of the strong anisotropy and deformability of the metal mesh, it was necessary to design and implement a machine that can guarantee a two-dimensional tensioning.

This equipment has been called T.A.S.T.I., which stands for Two Axial Stretch Test Instrument. On the device, it is possible to mount a sample of the mesh, up to 400x400 mm, which is grasped and pulled by adjustable hooks, anchored to sliding supports along very low friction guides. The machine can impose independent displacements along with two orthogonal directions while measuring the reaction forces. Through a PID control, it is also possible to apply loads on a given sequence. The displacement is applied through a system of cables and pulleys connected to two stepper motors, able to rotate at small step angles, while the reaction forces are measured through extensimetric load cells, Marotta et al. (2016).

Fig. 5 and Fig. 6 show the whole device and the load system, respectively.

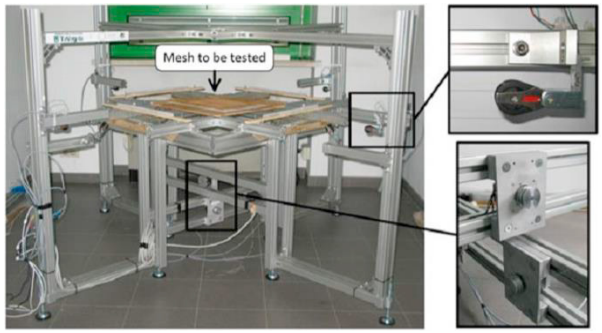

Fig. 5. T.A.S.T.I. machine

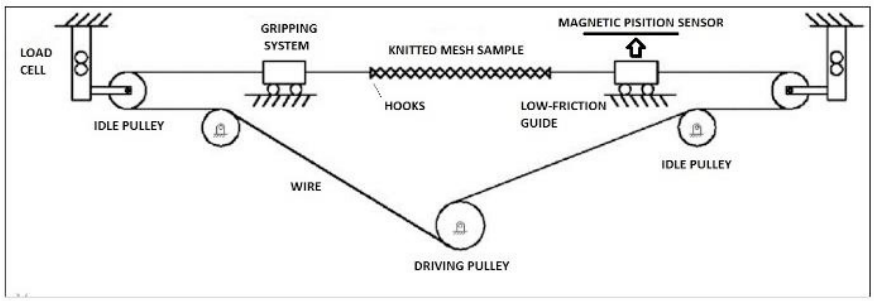

Fig. 6. Scheme of a single-direction loading system.

4.2. Description of the experimental system

A square mesh sample of approximately *15 cm* by side was installed on the machine as shown in Fig. 6. Even if the hooks were placed as regularly as possible to guarantee a uniform tensional state in the middle of the mesh, the areas near them were subjected to a non-regular distribution of loads, Valentini et al. (2016). To avoid this effect and to generate a stable and known constraint condition, the mesh was leaned on a circular support (lower than the side of the mesh). Thus, the vibrating surface considered is this circular portion of the mesh. To enlarge the image, two magnifying lenses were interposed between the net and the camera, parallel each other and at an appropriate distance to guarantee an optimal focus. See Fig. 7.

Fig. 7. T.A.S.T.I. machine with accessory instrumentation used.

The remaining equipment consisted of a led lamp, a camera capable to shoot up to *1500* frame per second, and a tripod on which this last is mounted. The lamp was placed above the net, so that the light hits directly the metal mesh without crossing the magnifying glasses and then coming back, causing unpleasant flicker when shooting. The tripod was set to form an angle of about 30 degrees between the line connecting net and camera, and an imaginary horizontal plane.

For the analysis of both free and forced vibration, the equipment just described is the same. However, a significant difference holds: the circular support must be still during the free vibration measurements, while on the contrary during forced vibrations the support itself confers the motion to the mesh sample (Fig. 8).

Therefore, for measuring free responses, the support was anchored to a wooden rigid panel and the initial perturbation is given by an instant pinch with a needle, while for measuring forced responses the support is integral to a shaker, able to vibrate within a wide range of frequencies, see Fig. 8.

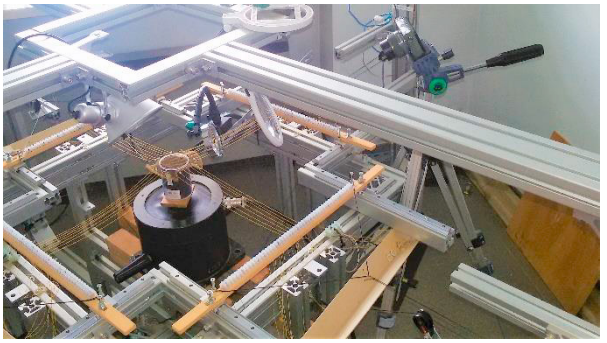

Fig. 8. Equipment assembly for forced vibration.

4.3. Description of the experimental procedure

For both analyses, the procedure is quite similar: 15 tests were performed, each of them with a larger imposed displacement on the mesh (in Test 1, stepper motor rotate of 1 degree, and so on). Each test requires four steps:

1. Pre-tensioning: the mesh is pre-tensioned with a low load to make sure that all hooks grasp the mesh and also to make the wires settle to avoid the dissipation of energy in the form of friction;
2. Tensioning: the tensioning state is maintained for a period that allows shooting the video;
3. Mesh excitement and video shooting:
   - 3.1. (free vibrations): when the net is loaded, the movie starts an instant before the mesh is pinched. The area of contact with the needle has to be as close as possible to the centre of the circular vibrating zone. If it were shifted, even slightly, vibrating modes different from the first one would be excited and any information obtained would be less reliable;
   - 3.2. (forced vibrations): the shaker is switched on, inducing vibrations in the mesh. The oscillation frequency, from zero, is progressively increased. The mesh vibrates at the set frequency with a low amplitude of oscillation, until the frequency approaches resonance: at this point, vibrations are wide enough to be visible to the naked eye, the frequency is kept at that value and the movie is shot. Then the shaker is switched off;
4. Unloading: the load is removed and the procedure can restart from step 1 for the subsequent test.

In each test, two orthogonal loads were measured by T.A.S.T.I. and frequencies of vibration extrapolated from videos by appropriate image analysis. Every value is reported in Table 1, concerning free vibrations, and Table 2, for forced vibrations.

4.4. Comparison between measured and calculated data

The first challenge regards which approximation is better to use.

The mesh cannot be considered as a simple two-dimensional object since its structure comprehends full areas and empty areas, repeated in space with particular shapes and dimensions. For that reason, it is necessary to provide adjustments, Soedel (2004).

Table 1. Free Vibration Tests.

Free Vibrations	Tension y (N)	Tension x (N)	Frequency (Hz)
TEST 1	0,5949	0,7574	215,6
TEST 2	0,6615	0,9285	253,1
TEST 3	0,8739	1,1082	274,2
TEST 4	0,9664	1,3080	293,0
TEST 5	1,2098	1,5213	321,1
TEST 6	1,4430	1,9424	360,9
TEST 7	1,5089	2,1910	377,3
TEST 8	1,6566	2,4470	400,8
TEST 9	1,9489	2,8765	435,9
TEST 10	2,1936	3,1873	459,4
TEST 11	2,7205	3,7222	503,9
TEST 12	2,7662	3,6379	501,6
TEST 13	3,0973	4,1613	539,1
TEST 14	3,5070	4,8904	574,2
TEST 15	3,7163	4,9212	581,3

Table 2. Forced Vibration Tests.

Forced Vibrations	Tension y (N)	Tension x (N)	Frequency (Hz)
TEST 1	0,4841	0,5875	189,8
TEST 2	0,6160	0,8112	201,6
TEST 3	0,6508	0,9557	236,7
TEST 4	0,9021	1,1435	271,9
TEST 5	1,1177	1,5428	316,4
TEST 6	1,2396	1,6420	330,5
TEST 7	1,3680	1,9045	349,2
TEST 8	1,6630	2,3700	389,1
TEST 9	1,8008	2,4993	405,5
TEST 10	2,1906	2,9680	440,6
TEST 11	2,2984	3,1790	461,7
TEST 12	2,3596	3,2773	459,4
TEST 13	3,0112	4,0710	520,3
TEST 14	3,0694	4,2602	522,7
TEST 15	3,2649	4,5612	550,8

On the other hand, it cannot even be considered as an ordinary one-dimensional object, because some information is inevitably lost. Even if reducing the problem to one dimension is possible, it encounters the necessity to overcome the obstacle of proportions between width and length, Weaver et al. (1990).

The approximation of the mesh to a one-dimensional object (vibrating wire) fits well to the measured data if a golden rectangle, inscribed in the edge circumference and under the influence of the highest tension alone, is considered.

A golden rectangle is a rectangle whose sides are in the golden ratio $r = \left(1+\sqrt{5}\right)/2$ between them.

Moreover, only the highest tension is considered because it represents the load in the stiffest direction, i.e. the one that contributes the most to the variation of potential (deformation) energy during vibrations. With these clarifications and making calculations, the first natural frequency fits the following (One Dimensional Approximation model):

$$\nu_1 \simeq \frac{1}{1.7013D}\sqrt{\frac{T_x}{0.5257\sigma D}} \simeq 0.8107\sqrt{\frac{T_x}{\sigma D^3}} \tag{6}$$

being the diameter D and the mass per unit area σ known data.

When considering the mesh as a two-dimensional object, the approximation of the circular net fits very well, if some adjustments are made. As previously said, analytical formulas in Paragraph 2 and 3 do not take into account neither the mesh strong anisotropy nor its complex geometry. So, two coefficients c_1 and c_2, that consider such aspects, have been introduced in the circular net formula:

$$\nu_{m,n} = \frac{c_1\left(\lambda a\right)_{m,n}}{2\pi r}\sqrt{\frac{c_2 T_x' + T_y'}{\sigma}} \tag{7}$$

These two coefficients are estimated with the least-squares method directly on the experimental data of free

vibrations, giving for the first natural frequency (Two Dimensional Approximation model):

$$\nu_1 \simeq \frac{0.5166}{D}\sqrt{\frac{2.4464T_x' + T_y'}{\sigma}} \tag{8}$$

Then, data from forced vibrations are used as a validation of formulas (6) and (8).

In Table 3 and Table 4, percentage errors between the measured frequencies and frequencies calculated in the approximation of One-dimensional (ODA) structure and two-dimensional (TDA) structure are given, for both free and forced vibrations.

Table 3. Free Vibration Tests. Frequencies calculated in one-dimensional approximation (ODA) and two-dimensional approximation (TDA) with relative percentage errors.

Test n.	Freq ODA (Hz)	Freq TDA (Hz)	% error ODA	% error TDA
1	222,529	228,292	3,21	5,89
2	246,383	249,592	-2,65	-1,39
3	269,166	276,287	-1,84	0,76
4	292,431	297,604	-0,19	1,57
5	315,372	324,082	-1,78	0,93
6	356,353	362,914	-1,26	0,56
7	378,475	381,801	0,31	1,19
8	399,974	402,658	-0,21	0,46
9	433,657	436,607	-0,51	0,16
10	456,485	460,463	-0,63	0,23
11	493,299	501,336	-2,10	-0,51
12	487,683	498,167	-2,77	-0,68
13	521,588	531,322	-3,25	-1,44
14	565,436	573,267	-1,53	-0,16
15	567,214	578,885	-2,42	-0,42

Table 4. Forced Vibration Tests. Frequencies calculated in one-dimensional approximation (ODA) and two-dimensional approximation (TDA) with relative percentage errors.

Test n.	Freq ODA (Hz)	Freq TDA (Hz)	% error ODA	% error TDA
1	186,860	196,052	-1,55	3,29
2	219,576	227,850	8,92	13,02
3	238,329	243,945	0,69	3,06
4	260,695	271,892	-4,12	0,00
5	302,811	312,323	-4,29	-1,29
6	312,404	323,925	-5,47	-1,99
7	336,442	346,636	-3,65	-0,73
8	375,320	385,564	-3,54	-0,91
9	385,420	397,250	-4,95	-2,03
10	420,012	434,230	-4,67	-1,45
11	434,684	448,220	-5,85	-2,92
12	441,350	454,855	-3,93	-0,99
13	491,901	508,692	-5,46	-2,23
14	503,203	518,645	-3,73	-0,78
15	520,677	536,214	-5,47	-2,65

Some notes arise:

a) both approximations are effective, but the two-dimensional one is often better.
b) for higher values of tensioning, the ODA tends to diverge from experimental frequencies (errors increase), this is due to neglecting one of the two loads, which becomes more affecting as soon as the loads increase;
c) apart from test 1, ODA presents always negative errors, this means that measured frequency is always smaller than experimental (real) frequency;
d) experimental values of Test 1 are less reliable than those of other tests. This is because with such low tension there is the risk that a higher percentage of the force measured by the load cells is due to frictions present in the network and in the T.A.S.T.I. machine, spoiling load data. This also explains the higher values of error;
e) The Test 2 included in Table 4 presents very high error values. This is due to the fact that because of inaccuracies during the test, the mesh was not in resonance when shooting. This explanation is validated by the amplitude of vibration, in Test 2 smaller than in the others.

5. Identification of mesh tensioning

With the explained method, it is possible to know the first natural frequency of the mesh, starting from loads applied. Since the goal was the inverse (to estimate tensions from the frequency), it is necessary to solve the reciprocal problem.

In one-dimensional approximation, this is very easy: it is sufficient to invert the formula and the main tension is uniquely determined. Moreover, according to point 3 of notes in paragraph 4.4, the resulting tension is always an excess estimate of the effective one.

Instead, in two-dimensional approximation, two unknown quantities are present in a single condition. To solve the tensioning status, i.e. to determine both tensions, an additional condition is required.

For example, as a first attempt, a plausible hypothesis could be that of uniformity of loads. Another is that of knowing the ratio between tensions, and so on…

In every case, it must be kept in mind the fact that one tension has a much larger effect than the other does on the vibration frequency since it contributes the most to the variation of deformation energy. Therefore, after having imposed the secondary condition, and so found tensions, the accuracy of the principal one is stricter.

In Fig. 9 and 10, two-dimensional trend ($frequency - T_x$) and three-dimensional trends ($frequency - T_x - T_y$) of both ODA and TDA are displayed, together with experimental values of free and forced vibrations tests. T_x is the tension in the direction of maximum stiffness, i.e. the most representative, T_y is the load in the direction orthogonal to the previous one.

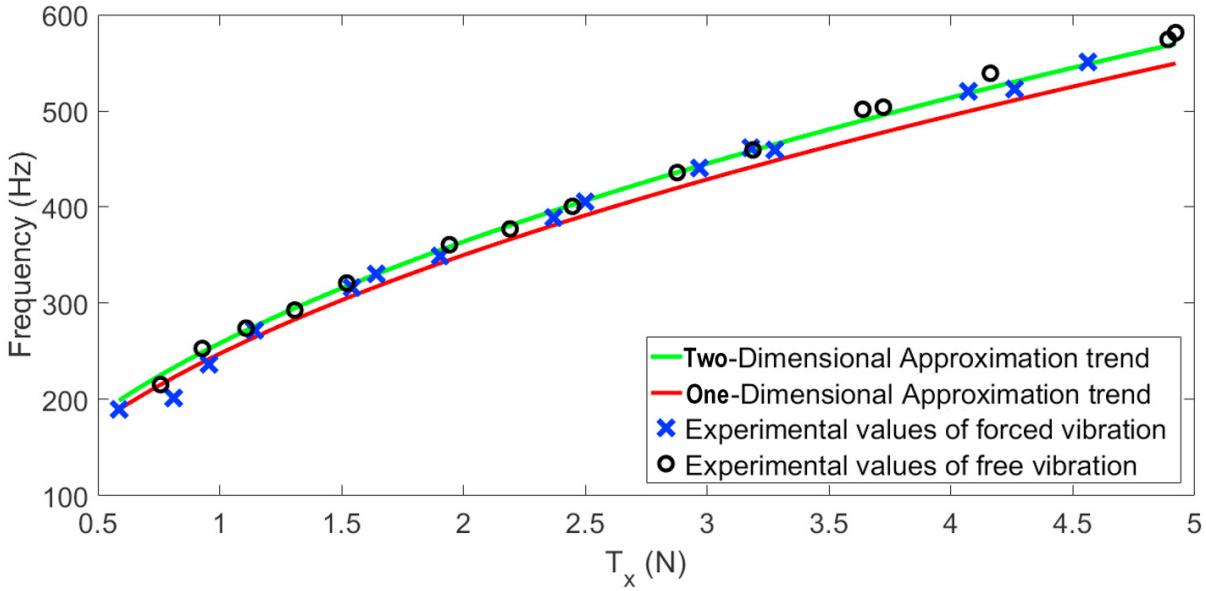

Fig. 9. Two-dimensional comparison of experimental data and expected trends.

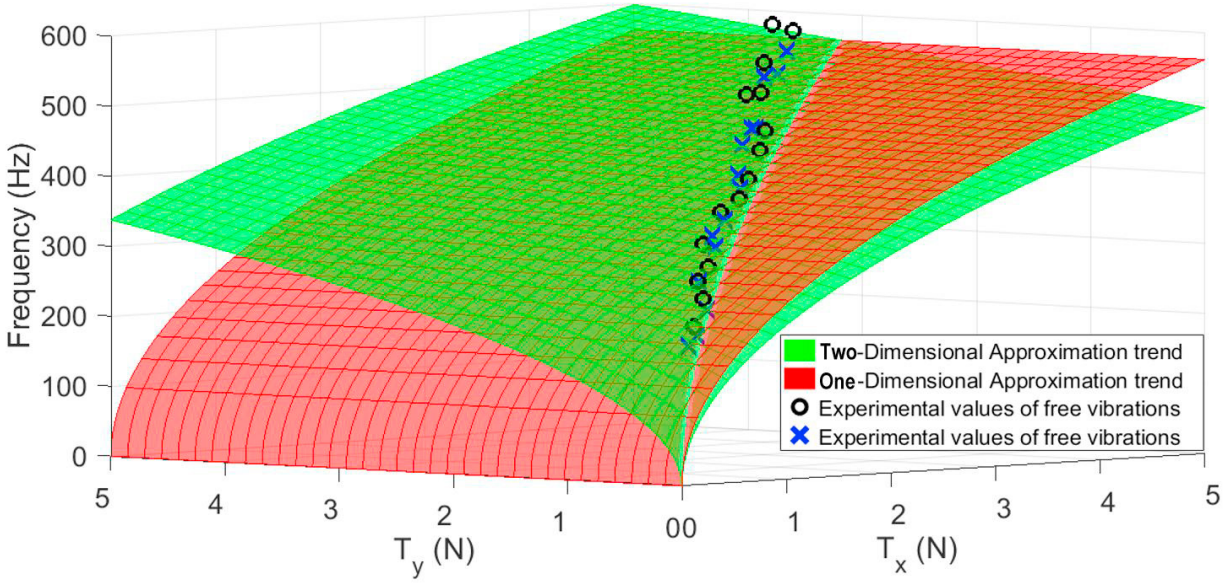

Fig. 10. Three-dimensional comparison of experimental data and expected trends.

6. Conclusions

In conclusion, thanks to this optical method, it has been possible to find an optimal experimental correlation between the tensioning status acting on the mesh and its first natural frequency, with satisfying approximation.

- To obtain acceptable results, being sure of the boundary constraints is mandatory, as well as exciting the desired mode of vibration;
- For the mesh under exam, although axial vibrations had the advantage to be virtually independent of the type of boundary conditions (i.e. type of link and shape of the mesh) since much more localized, they have such high frequency and damping that is impossible to appreciate them with the given camera;
- The predominant orthotropic direction makes possible to have quite good results already with the 1D approach;
- A two-dimensional simplified criterion has been introduced, generalizing existing models of the net;
- The technique requires the tuning of two coefficients, whose values need to be calibrated for the mesh under investigation;
- Measurements of both free and forced vibrations gave similar results. Anyway, it is worth to notice that free vibrations could be used on the mesh already installed on the reflector structure to have feedback on tensioning, while the forced ones are easier to reproduce in the laboratory and could be used to calibrate the coefficients in the 2D formula.

References

De Salvador, W., Marotta, E., Salvini, P., 2017. Strain Measurements on Compliant Knitted Mesh Used in Space Antennas, by means of 2D Fourier Analysis. Strain, Vol. 54, 1, 2018.

Marotta, E., De Salvador, W., Pennestrì, E., Salvini, P., Scialino, L., & Valentini, P. P., November 2016. Some problems arising during the experimental characterization of compliant knitted mesh. 37th Int. Esa Antenna workshop, Esa/Estec (pp. 15-17).

http://www.northropgrumman.com/BusinessVentures/AstroAerospace/Products/Documents/pageDocs/Parametrics.pdf, 2012.

http://www.northropgrumman.com/BusinessVentures/AstroAerospace/Products/Documents/pageDocs/AstroMesh_DataSheet.pdf, 2017.

Thomson M.W.,2000. The AstroMesh Deployable Reflector. In: Pellegrino S., Guest S.D. (eds) IUTAM-IASS Symposium on Deployable Structures: Theory and Applications. Solid Mechanics and Its Applications, vol 80. Springer, Dordrecht.

Thomson, M.W., Fang, H., Pearson, J., Moore, J., & Lin, J., September 2007. Prospects of large deployable reflector antennas for a new generation of geostationary Doppler weather radar satellites. In AIAA SPACE 2007 Conference & Exposition.

Thomson, M. W.. November 2008. Mechanical vs. inflatable deployable structures for large apertures or still no simple answers. In Large Space Apertures Workshop California Institute of Technology, Pasadena, California.

Soedel, W., (2004). Vibrations of shells and plates, New York, CRC Press.

Valentini,P.P., Falcone, M., Marotta, E., Pennestrì, E., Salvini, P.,2016. Theoretical and experimental characterization of a FEM element assembly for the simulation of very compliant knitted mesh . International Journal for Numerical Method in Engineering, Vol. 107, 419–429.

Weaver, Jr., W., Timoshenko, S. P., & Young, D. H., 1990. Vibration problems in engineering. New York, John Wiley & Sons.